Journal of Catalysis 330 (2015) 330–343

Contents lists available at ScienceDirect

Journal of Catalysis

journal homepage: www.elsevier.com/locate/jcat

Hydrodesulfurization of dibenzothiophene, 4,6-dimethyldibenzothiophene, and their hydrogenated intermediates over bulk tungsten phosphide

Lei Yang [a], Xiang Li [a,b,c,*], Anjie Wang [a,b,c], Roel Prins [d], Yongying Chen [a,b], Xinping Duan [a,e]

[a] State Key Laboratory of Fine Chemicals, School of Chemical Engineering, Dalian University of Technology, No. 2 Linggong Road, Dalian 116024, People's Republic of China
[b] Liaoning Key Laboratory of Petrochemical Technology and Equipments, Dalian University of Technology, No. 2 Linggong Road, Dalian 116024, People's Republic of China
[c] Penn State and Dalian University of Technology Joint Center for Energy Research (JCER), Dalian University of Technology, No. 2 Linggong Road, Dalian 116024, People's Republic of China
[d] Institute of Chemical and Bioengineering, ETH Zurich, 8093 Zurich, Switzerland
[e] Department of Chemistry, National Engineering Laboratory for Green Chemical Production of Alcohols, Ethers and Esters, Xiamen University, Xiamen 361005, People's Republic of China

ARTICLE INFO

Article history:
Received 30 April 2015
Revised 15 July 2015
Accepted 16 July 2015

Keywords:
Hydrodesulfurization
Dibenzothiophene
4,6-Dimethyldibenzothiophene
Hydrogenated intermediates
Tungsten phosphide
Piperidine

ABSTRACT

The kinetics of the hydrodesulfurization (HDS) of dibenzothiophene (DBT), 4,6-dimethyldibenzothiophene (4,6-DMDBT), and their hydrogenated intermediates over bulk tungsten phosphide (WP) was studied. WP possessed high hydrogenation/dehydrogenation activity but was highly sensitive to piperidine inhibition. 4,6-DMDBT reacted faster than DBT, and both DBT and 4,6-DMDBT reacted mainly through the hydrogenation pathway. The methyl groups suppressed the direct desulfurization of 4,6-DMDBT but significantly promoted the hydrogenation of 4,6-DMDBT and the dehydrogenation of 1,2,3,4-tetrahydro-4,6-dimethyldibenzothiophene (TH-4,6-DMDBT) and 1,2,3,4,4a,9b-hexahydro-4,6-dimethyldibenzothiophene, but decreased the rate of hydrogenation of TH-4,6-DMDBT. Piperidine inhibited the HDS of 4,6-DMDBT much more strongly than that of DBT. Substantial dehydrogenation of TH-4,6-DMDBT to 4,6-DMDBT and two of its isomers occurred. The formation of these 4,6-DMDBT isomers in the dehydrogenation of TH-4,6-DMDBT and the hydrocracking of 1-methyl-4-(3-methylcyclohexyl)-benzene, as well as the formation of cyclopentylphenylmethane and (cyclopentylmethyl)cyclohexane, is ascribed to the metallic character of WP.

1. Introduction

The metal-rich transition-metal phosphides (e.g., WP, MoP, Co_2P, CoP, Ni_2P) have attracted increasing attention as a novel class of hydrodesulfurization (HDS) catalysts, due to their high activity and stability under HDS conditions [1–3]. They are covalent compounds, in which the electron density is shared between the metal and phosphorus atoms [4]. The order of overall activity of the transition-metal phosphides in the simultaneous HDS of dibenzothiophene (DBT) and hydrodenitrogenation (HDN) of quinoline is $Fe_2P < CoP < MoP < WP < Ni_2P$, based on comparison with an equal number of sites as determined by CO chemisorption [5–7]. The most active (Ni_2P) and the second most active catalyst (WP) possess different structures. The crystal structure of Ni_2P is the same as that of Fe_2P, and the hexagonal unit cell contains one Ni atom in tetrahedral coordination and another Ni atom in square-pyramidal coordination [7]. Tungsten phosphide, on the other hand, adopts the orthorhombic manganese phosphide (MnP) structure, which is closely related to the hexagonal NiAs structure, but in which lattice distortions accompany the formation of chains of phosphorus atoms [8].

For the development and practical application of high-performance transition-metal phosphide HDS catalysts, an intensive study of the HDS reaction mechanism and kinetics of the most refractory sulfur-containing molecules, such as DBT and its alkylated derivatives (DBTs), over this new family of catalysts is needed. The HDS reaction networks of these molecules are complex and can be divided into two parallel pathways: direct desulfurization (DDS) and hydrogenation (HYD). DDS leads to the formation of biphenyls, while HYD yields not only the final desulfurized products cyclohexylbenzenes and bicyclohexyls, but

* Corresponding author at: State Key Laboratory of Fine Chemicals, School of Chemical Engineering, Dalian University of Technology, No. 2 Linggong Road, Dalian 116024, People's Republic of China. Fax: +86 411 84986121.
E-mail address: lixiang@dlut.edu.cn (X. Li).

http://dx.doi.org/10.1016/j.jcat.2015.07.019
0021-9517/

also tetrahydro (TH), hexahydro (HH), and dodecahydro (DH) sulfur-containing intermediates [9]. Therefore, the HDS reactions not only of the parent sulfur-containing molecules but also of their hydrogenated intermediates should be investigated. Previously, we studied the HDS of DBT and its hydrogenated intermediates, 1,2,3,4-tetrahydro-dibenzothiophene (TH-DBT) and 1,2,3,4,4a,9b-hexahydro-dibenzothiophene (HH-DBT), over bulk Ni_2P and MoP catalysts [10,11] and the HDS of 4,6-dimethyldibenzothiophene (4,6-DMDBT), 1,2,3,4-tetrahydro-4,6-dimethyldibenzothiophene (TH-4,6-DMDBT), and 1,2,3,4,4a,9b-hexahydro-4,6-dimethyldibenzothiophene (HH-4,6-DMDBT) over bulk Ni_2P [12]. Over Ni_2P, DBT mainly desulfurized by the DDS pathway, while desulfurization of 4,6-DMDBT occurred predominantly through the HYD pathway, and 4,6-DMDBT reacted much more slowly than DBT [10,12]. In addition to these results, which are in line with results obtained with sulfided Co–Mo and Ni–Mo catalysts [9,13], TH-4,6-DMDBT readily dehydrogenated to dimethyldibenzothiophene [12], whereas TH-DBT did not dehydrogenate to DBT under identical reaction conditions [10]. In the present work, we studied the HDS of these sulfur-containing molecules over bulk WP (tungsten phosphide). Since actual fuels contain not only sulfur-containing molecules, but also nitrogen-containing compounds, we studied the HDS in the presence of piperidine as a model nitrogen-containing compound. Our aim was to gain a deeper understanding of the HDS performance of WP, to determine the kinetics, and to investigate the inhibiting effect of piperidine.

2. Experimental methods

2.1. Preparation of DBT, 4,6-DMDBT, and their hydrogenated intermediates

DBT was synthesized as described in the literature [14]. TH-DBT was synthesized according to the method of DiCesare et al. [15],

Table 1
The structures and acronyms of the main compounds involved in the present work.

Name	Structure	Acronym
Dibenzothiophene	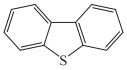	DBT
1,2,3,4-Tetrahydro-dibenzothiophene	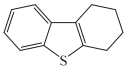	TH-DBT
1,2,3,4,4a,9b-Hexahydro-dibenzothiophene	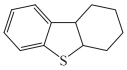	HH-DBT
Dodecahydro-dibenzothiophene	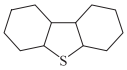	DH-DBT
Biphenyl	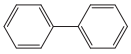	BP
Cyclohexylbenzene (phenylcyclohexane)	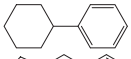	CHB
Cyclopentylphenylmethane	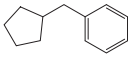	CPPM
Bi(cyclohexane)	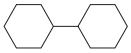	BCH
Cyclopentylcyclohexylmethane	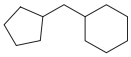	CPCM
4,6-Dimethyldibenzothiophene	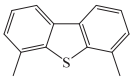	4,6-DMDBT
1,2,3,4-Tetrahydro-4,6-dimethyldibenzothiophene	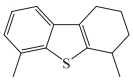	TH-4,6-DMDBT
1,2,3,4,4a,9b-Hexahydro-4,6-dimethyldibenzothiophene	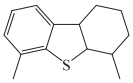	HH-4,6-DMDBT
Dodecahydro-4,6-dimethyldibenzothiophene	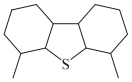	DH-4,6-DMDBT
3,3′-Dimethylbiphenyl	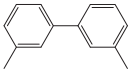	DM-BP
1-Methyl-3-(3-methylcyclohexyl)-benzene	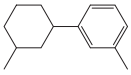	DM-CHB
1-Methyl-4-(3-methylcyclohexyl)-benzene	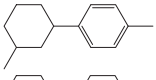	3,4′-DM-CHB
3,3′-Dimethylbi(cyclohexane)		DM-BCH
1-Phenyl-1-cyclohexene	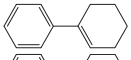	1-PCHE
3-Phenyl-1-cyclohexene	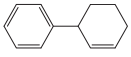	3-PCHE

with 2-bromocyclohexanone instead of 2-chlorocyclohexanone in the first step. A mixture of 4,6-DMDBT and TH-4,6-DMDBT was prepared by coupling 2-bromo-3-methyl-2-cyclohexen-1-one with 2-methylbenzenethiol and annulating the product with the aid of polyphosphoric acid [16]. After separation by silica gel column chromatography, 4,6-DMDBT was obtained as white needle-like crystals and TH-4,6-DMDBT as a colorless liquid [16]. HH-DBT [17] and HH-4,6-DMDBT [16] were produced by hydrogenation of TH-DBT and TH-4,6-DMDBT, respectively, with zinc and trifluoroacetic acid at room temperature.

2.2. Preparation of tungsten phosphide catalyst precursor

Tungsten phosphate was prepared by adding an aqueous solution of 1.5 g $(NH_4)_2HPO_4$ in 10 mL deionized water dropwise to a solution of 3.0 g $(NH_4)_6W_{12}O_{39}{\cdot}xH_2O$ in 15 mL deionized water under stirring. The resulting clear solution was stirred and evaporated to dryness, then dried at 120 °C for 12 h and calcined at 500 °C for 3 h to obtain the final oxidic precursor, which had a composition of $WO_3{\cdot}0.5P_2O_5$. The P/W and O/W molar ratios were 1.0 and 5.5, respectively.

2.3. HDS activity measurement

The catalytic reactions were carried out in a stainless steel tubular reactor (i.d. 8.0 mm). The oxidic precursor was pelleted, crushed, and sieved to 20–30 mesh. Prior to the HDS reaction, the precursor (0.10 g) was transformed into bulk WP by temperature-programmed reduction under 1.0 MPa in a 150 mL/min H_2 flow by heating from room temperature to 120 °C at a heating rate of 10 °C/min and keeping this temperature for 1 h, then heating to 400 °C at 5 °C/min, and finally heating at 1 °C/min to 650 °C and holding at 650 °C for 2 h.

After the precursor had been converted to the active WP phase, the reactor was cooled to the reaction temperature of 340 °C and the total pressure was increased to 4.0 MPa. The feed consisted of 1 kPa reactant (DBT, TH-DBT, HH-DBT, 4,6-DMDBT, TH-4,6-DMDBT, or HH-4,6-DMDBT), 165 kPa decalin (as solvent), and about 3.8 MPa H_2. In some experiments, 0.2 kPa piperidine (Sinopharm Chemical Reagent Co., Ltd.) was added. Weight time [18] was defined as $\tau = w_{cat}/n_{feed}$, where w_{cat} denotes the catalyst weight and n_{feed} the total molar flow to the reactor (1 g min/mol = 0.15 g h/L). The weight time was changed by varying the flow rates of the liquid (ranging from 0.05 to 0.3 mL/min) and gas, while keeping their ratio constant. The correspondence between the weight time τ and contact time τ_c is 1 g min/mol = 1.44×10^{-4} s. The contact time is defined as $\tau_c = (w_{cat} \cdot n_{site})/n_{feed}'$, where n_{feed}' is the molar flow rate of the reactant (excluding solvent), and n_{site} is the number of sites titrated by CO chemisorption (μmol/g).

The hydrogenation reactions of 1 kPa biphenyl (BP, Sinopharm Chemical Reagent Co., Ltd.) and 1 kPa cyclohexylbenzene (phenylcyclohexane, CHB, Acros) in the presence of 0.5 kPa benzothiophene (BT), as well as the hydrogenation reactions of 1 kPa 3,3′-dimethylbiphenyl (DM-BP, Tokyo Chemical Industry Co., Ltd.) and 1 kPa 1-methyl-4-(3-methylcyclohexyl)-benzene (3,4′-DM-CHB) in the presence of 0.5 kPa DBT, were carried out over WP under conditions identical to the HDS reactions described above. 3,4′-DM-CHB was synthesized by alkylation of toluene with 3-methylcyclohexanol in concentrated sulfuric acid [19]. All the reaction products were analyzed off line by an Agilent-6890N gas chromatograph equipped with a HP-5 column. Mass spectra were recorded on a GC–MS instrument (Agilent-7890A GC/7000B MS). The structures and the acronyms of the main compounds involved in the present study was listed in Table 1.

2.4. Catalyst characterization and density functional theory calculations

For characterization, a bulk WP sample was prepared under the same conditions as used in in situ reduction, followed by passivation with 0.5% (volume) O_2 in Ar. The X-ray diffraction (XRD) pattern of the passivated WP catalyst was measured on a Rigaku D/Max 2400 diffractometer with nickel-filtered Cu Kα radiation at 40 kV and 100 mA. Nitrogen physisorption was performed on a Quantachrome Autosorb-1-MP analyzer. The X-ray photoelectron spectroscopy (XPS) spectra were obtained with a Multilab 2000 X-ray photoelectron spectrometer using a Mg Kα source. For the individual energy regions, a pass energy of 20 eV was used. All binding energies were referenced to the C1*s* peak at 284.6 eV. Transmission electron microscopy (TEM) images were taken using a Tecnai G220 S-Twin microscope. CO adsorption was measured using pulsed chemisorption [20]. NH_3 temperature-programmed desorption (NH_3-TPD) of the bulk WP catalyst and, for comparison, of fumed silica (specific surface area 282 m^2/g) was carried out on a Chembet-3000 analyzer. Prior to the NH_3-TPD experiment, 0.2 g passivated WP catalyst sample was re-reduced in H_2 for 2 h at 500 °C and was then cooled to 30 °C and exposed to NH_3 for 30 min. After the reactor was purged in a He flow, the temperature was raised at a linear rate of 10 °C/min to 500 °C. Before the NH_3-TPD experiment with fumed silica, the silica was first dried at 120 °C for 2 h.

The thermodynamics of the interconversion between DBT and TH-DBT and between 4,6-DMDBT and TH-4,6-DMDBT under standard conditions was calculated using density functional theory (DFT) at the B3LYP level with a 6-31G* basis set. The calculations were performed with the Gaussian 03 program [21].

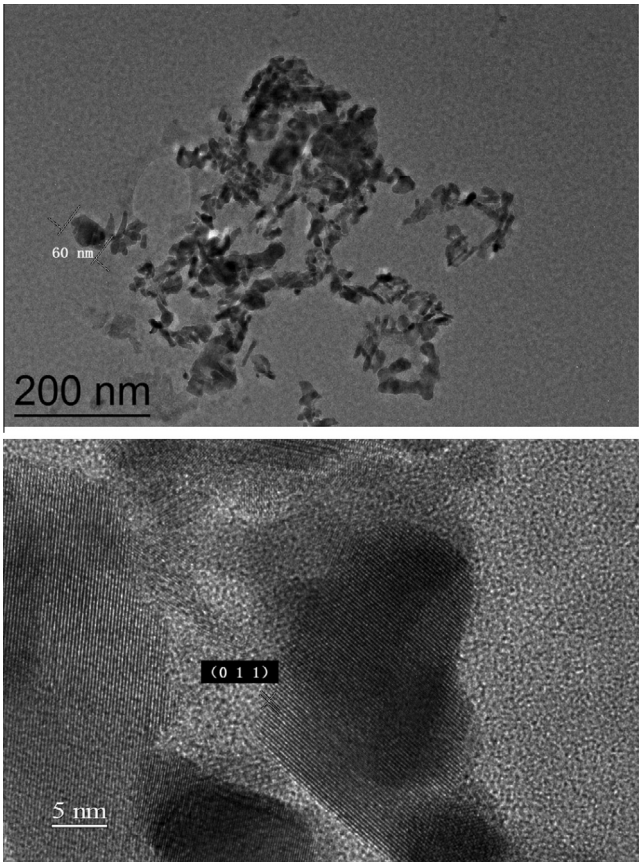

Fig. 1. TEM images of the bulk WP catalyst.

3. Results

3.1. Characterization

The XRD pattern of the WP catalyst (Fig. S1 in the Supplementary Material) showed that tungsten phosphide had formed by the reduction of the oxidic precursor. The CO uptake of the prepared WP was 2.4 μmol/g. The XPS spectra of the bulk WP catalyst in the binding energy regions of W4*f* and P2*p* are shown in Fig. S2 (Supplementary Material). The W4*f* spectrum consists of two split peaks due to spin–orbit interaction (W4$f_{7/2}$ and W4$f_{5/2}$), with a separation of 2.18 eV, an intensity ratio of 0.78, and a width ratio of 1.0 [22]. For the bulk WP sample, the major doublet, with a separation (2.1 eV) close to the theoretical one located at 31.0 eV (W4$f_{7/2}$) and 33.1 eV (W4$f_{5/2}$), can be attributed to $W^{\delta+}$ species ($0 < \delta \leqslant 4$) (Fig. S2A), which is related to the tungsten species in the WP phase [23]. The doublet associated with W^{6+} at 35.5 eV (W4$f_{7/2}$) and 37.5 eV (W4$f_{5/2}$) was also detected, with a very low intensity (Fig. S2A). The oxidation is due to air exposure of the sample before XPS analysis [23]. The doublet in the P2*p* region at 128.9 and 129.8 eV (Fig. S2B) shows that the P species in the surface of bulk WP can be assigned to P bonded to W in the form of a phosphide [24]. Because of the covalent nature of WP [4], the binding energy locations of W and P are near the elemental values [23]. The surface P/W atomic ratio determined by XPS was 0.85, indicating that the surface of the prepared WP catalyst was slightly metal-rich relative to the stoichiometric value (1.0). This is probably due to the loss of P at elevated temperature during the reduction [25]. The TEM images (Fig. 1) demonstrate that the WP particles were heterogeneously distributed with particle size range up to 60 nm. At higher resolution, the lattice fringes with an interplanar distance of 0.29 nm, corresponding to the (0 1 1) plane of WP, can be clearly observed, confirming the formation of the WP phase. The TEM images also indicate that the bulk WP catalyst is not a porous material. Therefore, the specific surface area and the pore volume of WP were only 8.8 m^2/g and 0.05 cm^3/g, respectively. Its micropore volume was almost zero. The NH_3-TPD profiles of bulk WP and fumed silica (the reference) both showed a faint peak (Fig. S3 in the Supplementary Material). Because silica has no measureable acidity, the weak peak with an onset temperature close to 120 °C must be due to the desorption of physisorbed NH_3. Thus, the comparison of the NH_3-TPD profile of bulk WP with that of fumed silica indicates that bulk WP catalyst has a low acidity.

3.2. Hydrodesulfurization of DBT and 4,6-DMDBT

The products of the reaction of DBT over bulk WP were BP, the product of the DDS pathway, TH-DBT and HH-DBT, the

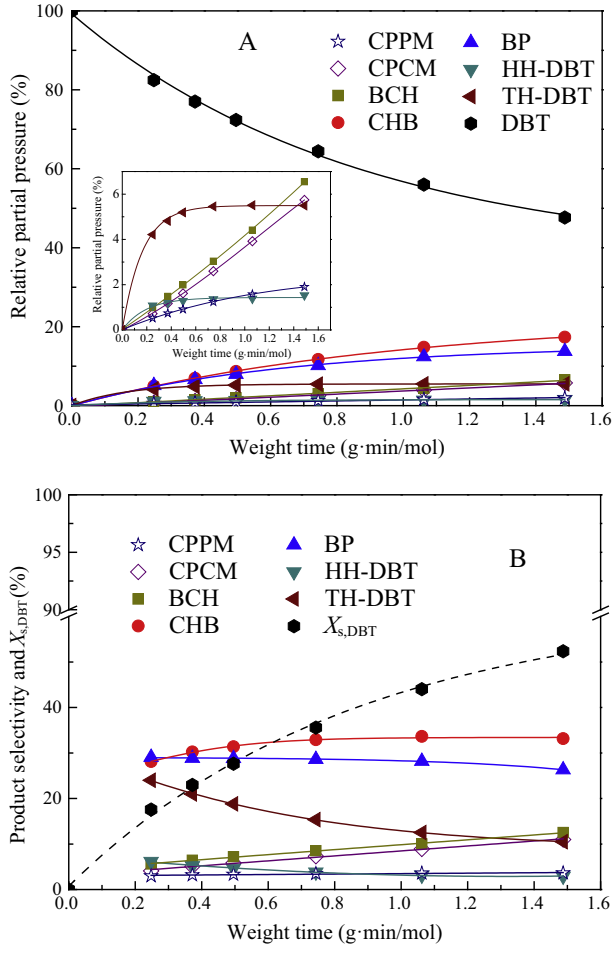

Fig. 2. HDS of DBT over bulk WP at 340 °C and 0 kPa piperidine as a function of weight time. (A) Relative partial pressures of the reactant and products. (B) The conversion of DBT ($X_{s,DBT}$, dashed line) and the product selectivities (solid lines). The inset in (A) shows the yield–time dependencies of TH-DBT, CPCM, BCH, HH-DBT, and CPPM in the relative partial pressure range from 0% to 7%. The lines in this figure and the following figures are simple connecting lines but not model fits.

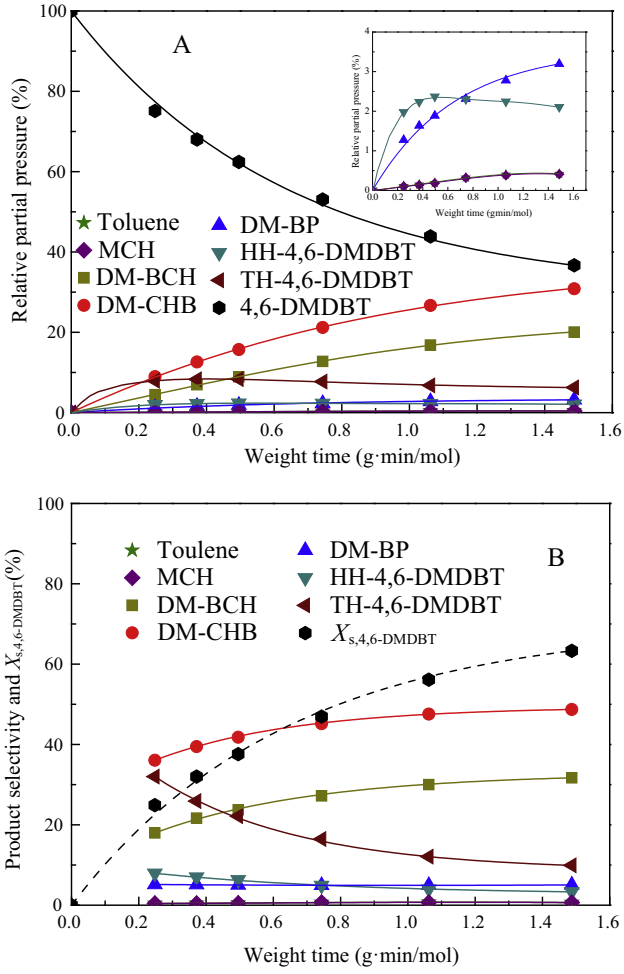

Fig. 3. HDS of 4,6-DMDBT over bulk WP at 340 °C and 0 kPa piperidine as a function of weight time. (A) Relative partial pressures of the reactant and products. (B) The conversion of 4,6-DMDBT ($X_{s,4,6\text{-DMDBT}}$, dashed line) and the product selectivities (solid lines). The inset in (A) shows the yield–time dependencies of HH-4,6-DMDBT, DM-BP, toluene, and MCH in the relative partial pressure range from 0% to 4%.

intermediates of the HYD pathway, and CHB and bi(cyclohexane) (BCH), the final products of the HYD pathway. Furthermore, substantial amounts of cyclopentylphenylmethane (CPPM) and cyclopentylcyclohexylmethane (CPCM) were observed, with yields comparable to those for HH-DBT and BCH, respectively (Fig. 2A). The yields of TH-DBT at $\tau = 0.74$, 1.1, and 1.5 g min/mol were 5.4%, 5.6%, and 5.4%, respectively (Fig. 2A). Although slowly, the yield–time curve of TH-DBT did pass through the maximum and started to decrease at $\tau > 1.1$ g min/mol, indicating that TH-DBT is an intermediate in the HDS of DBT. It is also a primary product, because its selectivity increased with decreasing weight time and extrapolated to a nonzero value at $\tau = 0$ g min/mol (Fig. 2B). CHB was the most abundant and BP the second most abundant product. They had comparable yields and selectivities. The BP selectivity decreased slowly from 29.1% at $\tau = 0.25$ g min/mol to 26.3% at $\tau = 1.5$ g min/mol (Fig. 2B). The result shows that the HDS of DBT over WP mainly follows the HYD route, and that BP reacts further.

Seven products were observed in the HDS of 4,6-DMDBT (Fig. 3): DM-BP, the product of the DDS pathway, TH-4,6-DMDBT and HH-4,6-DMDBT, the intermediates of the HYD pathway, 1-methyl-3-(3-methylcyclohexyl)-benzene (DM-CHB) and 3,3′-dimethylbi(cyclohexane) (DM-BCH), the final products of the HYD pathway, and small amounts of toluene and methylcyclohexane (MCH). The ratio of toluene to MCH was one, and the yield of each compound was less than 0.5% at $\tau = 1.5$ g min/mol (Fig. 3A). The reactivity of 4,6-DMDBT was higher than that of DBT. At $\tau = 1.5$ g min/mol, the conversion of 4,6-DMDBT was 63.3% (Fig. 3B), 10% higher than that of DBT (52.4%) (Fig. 2B). DM-CHB and DM-BCH were the most abundant and the second most abundant product, respectively. Their total selectivity at $\tau = 1.5$ g min/mol reached 80.4% (Fig. 3B). The yield of DM-BP was low (less than 3.2%, Fig. 3A). Its selectivity was only 5% and was almost independent of weight time, demonstrating that the HYD pathway dominates the HDS of 4,6-DMDBT. The low DDS reactivity of 4,6-DMDBT is due to the steric hindrance of the methyl groups at the 4 and 6 positions, which are close to the sulfur atom and prevent the σ-binding of the sulfur atom with the catalytic site [13]. The selectivities to TH-4,6-DMDBT and HH-4,6-DMDBT decreased with increasing weight time and were low at high weight time, indicating that these intermediates reacted quickly to the desulfurized products.

Piperidine strongly inhibited the reaction of DBT. At $\tau = 1.5$ g min/mol, the conversion of DBT decreased drastically from 52.4% in the absence of piperidine (Fig. 2B) to 10.5% in the presence of 0.2 kPa piperidine (Fig. 4B). BP was the most abundant product, and its selectivity at $\tau = 1.5$ g min/mol increased from 26.3% in the absence of piperidine to 51% in the presence of piperidine (Fig. 4B). Piperidine decreased the yields of CHB and BCH significantly. Consequently, TH-DBT became the second most abundant product (Fig. 4). No CPPM or CPCM was observed after the addition of piperidine.

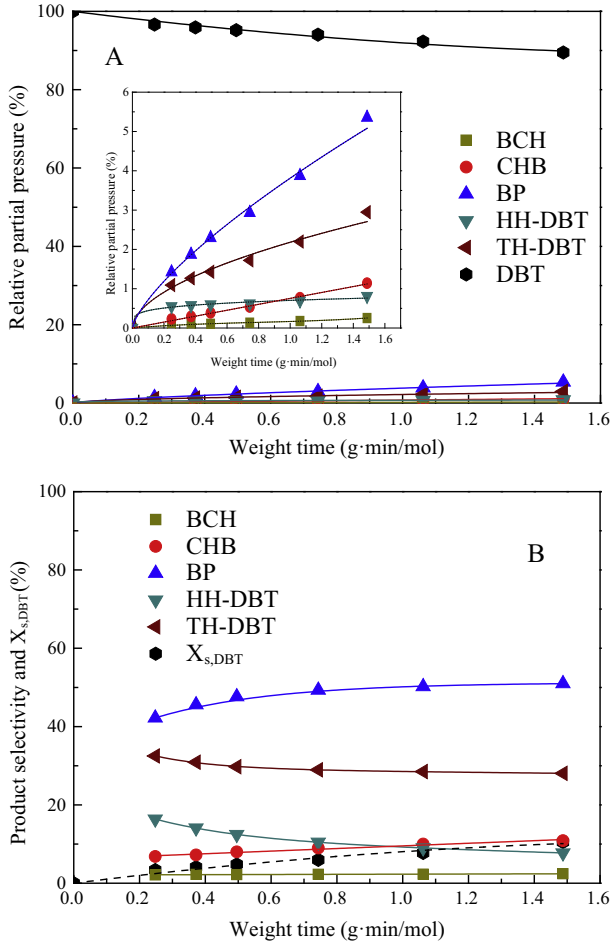

Fig. 4. HDS of DBT over bulk WP at 340 °C and 0.2 kPa piperidine as a function of weight time. (A) Relative partial pressures of the reactant and products. (B) The conversion of DBT ($X_{s,DBT}$, dashed line) and the product selectivities (solid lines). The inset is the amplified (A) in the relative partial pressure range from 0% to 6%.

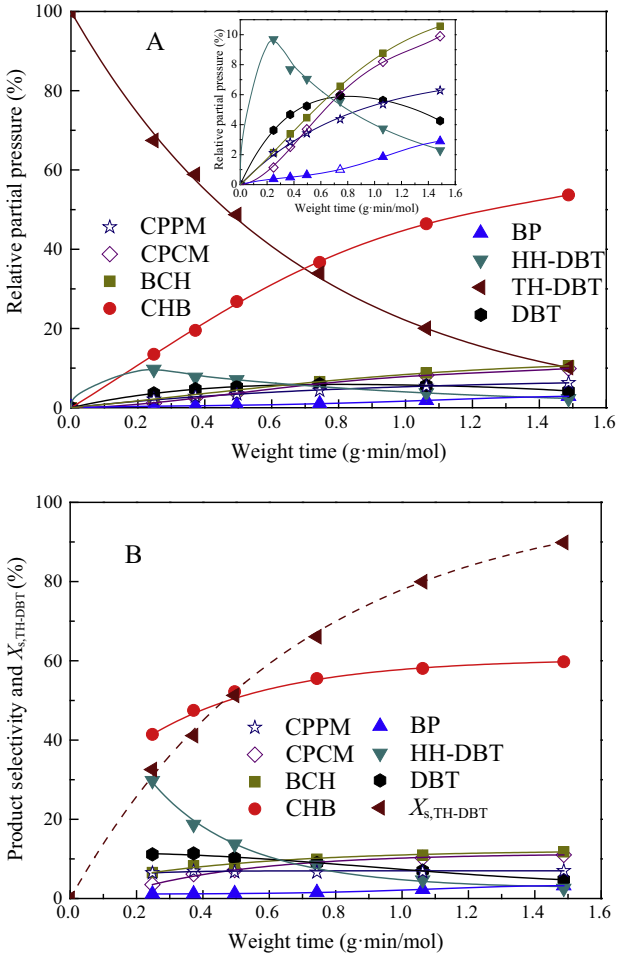

Fig. 5. HDS of TH-DBT over bulk WP at 340 °C and 0 kPa piperidine as a function of weight time. (A) Relative partial pressures of the reactant and products. (B) The conversion of TH-DBT ($X_{s,TH-DBT}$, dashed line) and the product selectivities (solid lines). The inset is the amplified (A) in the relative partial pressure range from 0% to 11%.

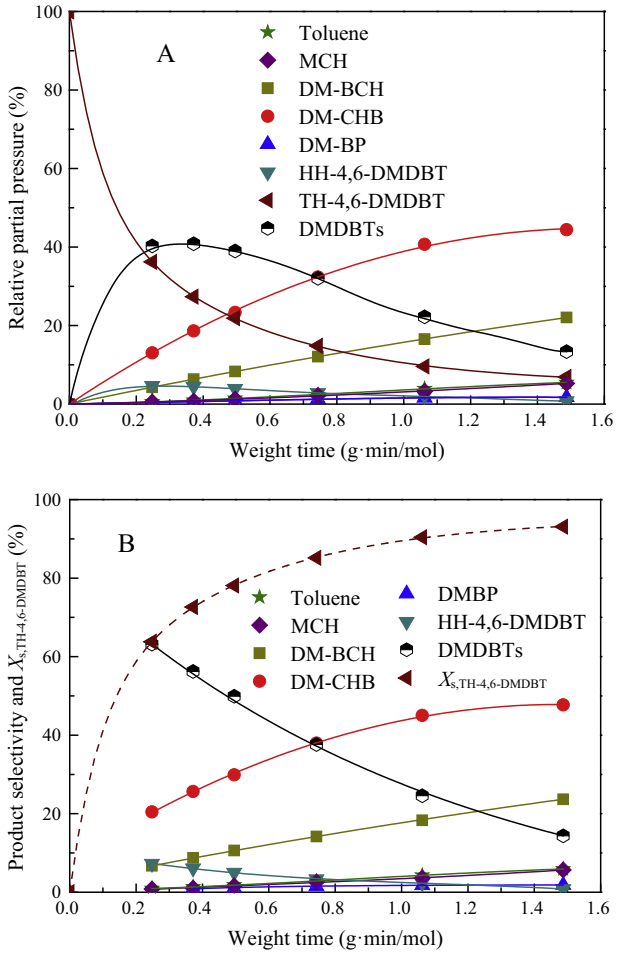

Fig. 6. HDS of TH-4,6-DMDBT over bulk WP at 340 °C and 0 kPa piperidine as a function of weight time. (A) Relative partial pressures of the reactant and products. (B) The conversion of TH-4,6-DMDBT ($X_{s,TH\text{-}4,6\text{-}DMDBT}$, dashed line) and the product selectivities (solid lines).

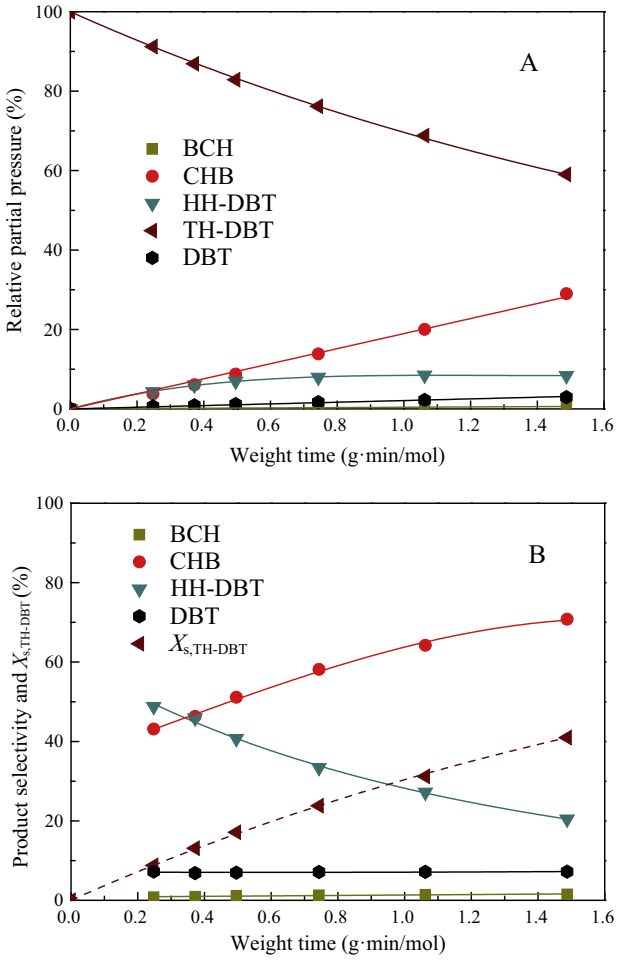

Fig. 7. HDS of TH-DBT over bulk WP at 340 °C and 0.2 kPa piperidine as a function of weight time. (A) Relative partial pressures of the reactant and products. (B) The conversion of TH-DBT ($X_{s,TH\text{-}DBT}$, dashed line) and the product selectivities (solid lines).

Piperidine inhibited the HDS of 4,6-DMDBT more strongly than the HDS of DBT. The conversion of 4,6-DMDBT was completely inhibited below $\tau = 1.1$ g min/mol, and at $\tau = 1.5$ g min/mol (the highest weight time studied), only 5.2% conversion of 4,6-DMDBT was obtained, with TH-4,6-DMDBT as the only product. The conversion of piperidine was almost complete at $\tau = 1.5$ g min/mol (Fig. S4 in the Supplementary Material). This means that 4,6-DMDBT cannot start to react until the piperidine concentration is low.

3.3. Hydrodesulfurization of TH-DBT and TH-4,6-DMDBT

TH-DBT reacted much faster than DBT, and its conversion reached 90% at $\tau = 1.5$ g min/mol (Fig. 5B). Besides the hydrogenation of TH-DBT to HH-DBT and the desulfurization of both TH-DBT and HH-DBT to CHB, BCH, CPPM, and CPCM, TH-DBT also dehydrogenated to DBT. CHB was the predominant product. While HH-DBT and DBT are intermediates and primary products of the HDS of TH-DBT, their yields passed through maxima at $\tau = 0.25$ and 0.74 g min/mol, respectively (Fig. 5A), while their selectivities decreased with weight time and were unequal to zero at $\tau = 0$ g min/mol (Fig. 5B). The yields of BCH, CPCM, and CPPM (Fig. 5) were higher when TH-DBT was the reactant than when DBT was the reactant (Fig. 2). A small amount of BP was detected as a final product (Fig. 5).

TH-4,6-DMDBT reacted faster than TH-DBT. At $\tau = 0.25$ g min/mol, its conversion was already 63.8% (Fig. 6B), about two times larger than that of TH-DBT (32.5%, Fig. 5B). The major product at $\tau < 0.74$ g min/mol was a mixture of three dimethyldibenzothiophene isomers (DMDBTs): 4,6-DMDBT, 2,6-dimethyldibenzothiophene (2,6-DMDBT), and another, unknown isomer with mass 212. According to our previous work [12], this isomer is most likely 3,6-dimethyldibenzothiophene (3,6-DMDBT). At $\tau = 1.5$ g min/mol, 4,6-DMDBT was the major isomer and represented 88% of the DMDBTs (Table S1 in the Supplementary Material). The selectivity to 3,6-DMDBT was 10%, while that to 2,6-DMDBT was only 2%. DMDBTs and TH-4,6-DMDBT tended to equilibrium with a DMDBTs/TH-4,6-DMDBT ratio of 1.9 at $\tau = 1.5$ g min/mol. At $\tau > 0.74$ g min/mol, DM-CHB was the most abundant product (Fig. 6A), and DM-BCH became the second most abundant product, at $\tau = 1.5$ g min/mol (Fig. 6), with a much higher yield than that of BCH in the HDS of TH-DBT (Fig. 5). HH-4,6-DMDBT showed a low yield. Both the yield–time and selectivity–time dependencies indicated that HH-4,6-DMDBT and DMDBTs were the primary products and intermediates in the HDS of TH-4,6-DMDBT (Fig. 6). The other minor desulfurization products observed were toluene and MCH, with a ratio close to 1 (Fig. 6).

The conversion of TH-DBT was only 41% at $\tau = 1.5$ g min/mol in the presence of 0.2 kPa piperidine (Fig. 7B). HH-DBT was the main product at $\tau < 0.37$ g min/mol, while CHB became the most abundant product as weight time increased (Fig. 7). The formation of BCH and DBT was strongly suppressed by piperidine. No CPPM or CPCM was detected after the addition of piperidine.

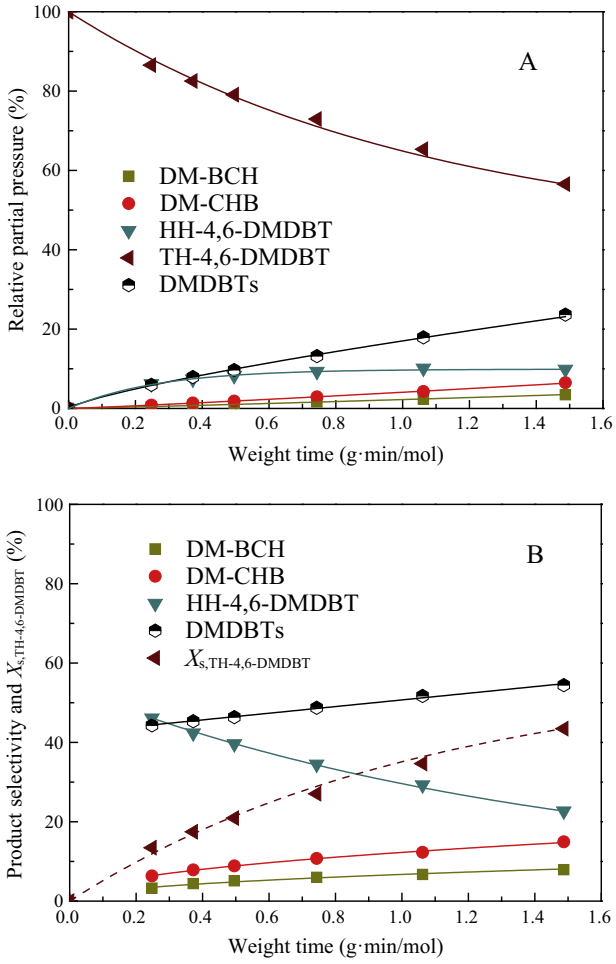

Fig. 8. HDS of TH-4,6-DMDBT over bulk WP at 340 °C and 0.2 kPa piperidine as a function of weight time. (A) Relative partial pressures of the reactant and products. (B) The conversion of TH-4,6-DMDBT ($X_{s,TH\text{-}4,6\text{-}DMDBT}$, dashed line) and the product selectivities (solid lines).

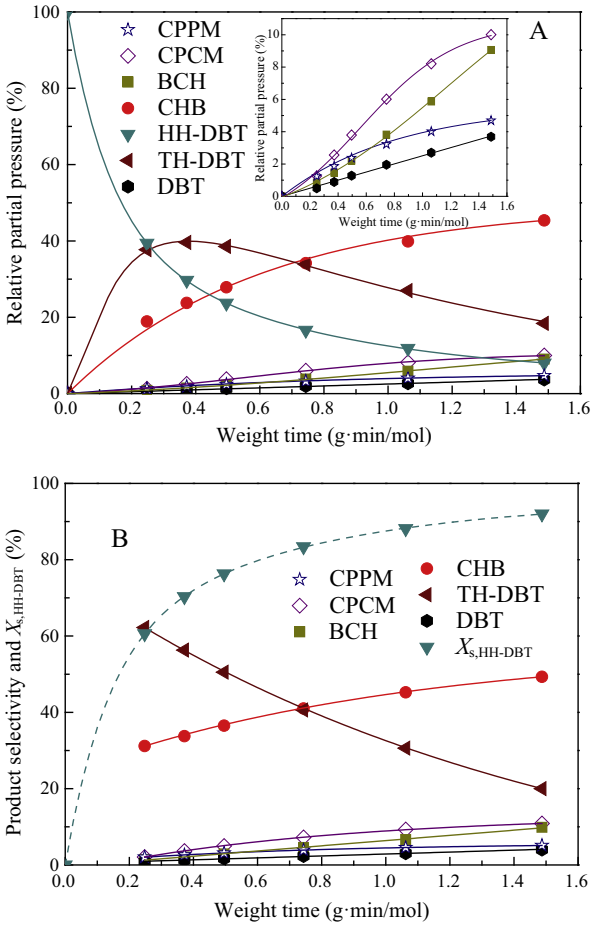

Fig. 9. HDS of HH-DBT over bulk WP at 340 °C and 0 kPa piperidine as a function of weight time. (A) Relative partial pressures of the reactant and products. (B) The conversion of HH-DBT ($X_{s,HH\text{-}DBT}$, dashed line) and the product selectivities (solid lines). The inset in (A) shows the yield–time dependencies of CPCM, BCH, DBT, and CPPM in the relative partial pressure range from 0% to 11%.

Piperidine decreased the conversion of TH-4,6-DMDBT more strongly than that of TH-DBT, from 63.8% in the absence of piperidine (Fig. 6B) to 13.4% in the presence of piperidine (Fig. 8B) at τ = 0.25 g min/mol. The decrease (50%) was about twice that observed in the HDS of TH-DBT (23%) (Figs. 5 and 7). Only four products (DMDBTs, HH-4,6-DMDBT, DM-CHB, and DM-BCH) were detected. The low yields and selectivities of DM-CHB and DM-BCH indicated that the desulfurization reactions were more inhibited by piperidine than the dehydrogenation/hydrogenation of TH-4,6-DMDBT. Although the yield of the DMDBTs was significantly lower in the presence of piperidine, it was still the most abundant product (Fig. 8). However, its yield–time and selectivity–time curves changed substantially (cf. Figs. 6 and 8) because piperidine slowed down the formation of DMDBTs, so that the maximum in the yield–time curve was not reached yet at the highest weight time. The selectivities of 2,6-DMDBT and 3,6-DMDBT decreased and thus the selectivity of 4,6-DMDBT increased (Table S1 in the Supplementary Material). The addition of piperidine did not change the features of the yield–time and selectivity–time curves of HH-4,6-DMDBT except for an increase in its yield and selectivity (cf. Figs. 6 and 8).

3.4. Hydrodesulfurization of HH-DBT and HH-4,6-DMDBT

HH-DBT reacted fast over WP and its conversion reached 92% at τ = 1.5 g min/mol (Fig. 9B). TH-DBT was the main product up to τ = 0.74 g min/mol, and thereafter CHB became the most abundant one (Fig. 9A). TH-DBT was a primary product, because its selectivity decreased with weight time and was unequal to zero at τ = 0 g min/mol (Fig. 9B), and its yield passed through a maximum at τ = 0.37 g min/mol, because it reacted further. The dehydrogenation of TH-DBT to DBT occurred, but the very low yield of DBT (Fig. 9A) demonstrates that the reaction was slow. TH-DBT and HH-DBT tended to equilibrium with a TH-DBT/HH-DBT ratio of 2.3 at τ = 1.5 g min/mol. The distributions of the hydrocarbon products (CHB, BCH, CPPM, and CPCM) (Fig. 9) were similar to those observed in the HDS of TH-DBT (Fig. 5).

HH-4,6-DMDBT reacted faster than HH-DBT. At low weight time, DMDBTs and TH-4,6-DMDBT were the most abundant and the second most abundant product, respectively (Fig. 10). The variations of the relative partial pressures and selectivities of DM-CHB, DM-BCH, toluene, and MCH with weight time (Fig. 10) were almost identical to those in the reaction of TH-4,6-DMDBT (Fig. 6), suggesting that the dehydrogenation/hydrogenation reactions between HH-4,6-DMDBT, TH-4,6-DMDBT, and DMDBTs are faster than their desulfurization. Neither DM-BP nor dodecahydro-4,6-dimethyldibenzothiophene (DH-4,6-DMDBT, the fully hydrogenated intermediate) was detected in the HDS of HH-4,6-DMDBT.

Piperidine decreased the conversion of HH-DBT and HH-4,6-DMDBT to 72.5% (Fig. 11B) and 72.2% (Fig. 12B) at τ = 1.5 g min/mol, respectively. Only TH-DBT, CHB, and BCH were detected in the reaction of HH-DBT at 0.2 kPa piperidine (Fig. 11). In the reaction of HH-4,6-DMDBT after the addition of

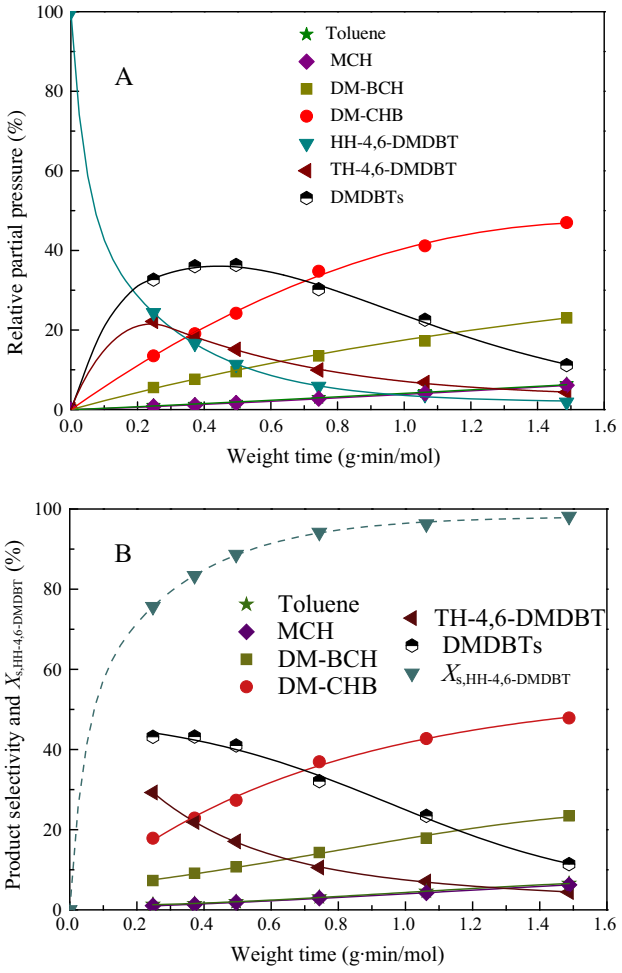

Fig. 10. HDS of HH-4,6-DMDBT over bulk WP at 340 °C and 0 kPa piperidine as a function of weight time. (A) Relative partial pressures of the reactant and products. (B) The conversion of HH-4,6-DMDBT ($X_{s,HH\text{-}4,6\text{-}DMDBT}$, dashed line) and the product selectivities (solid lines).

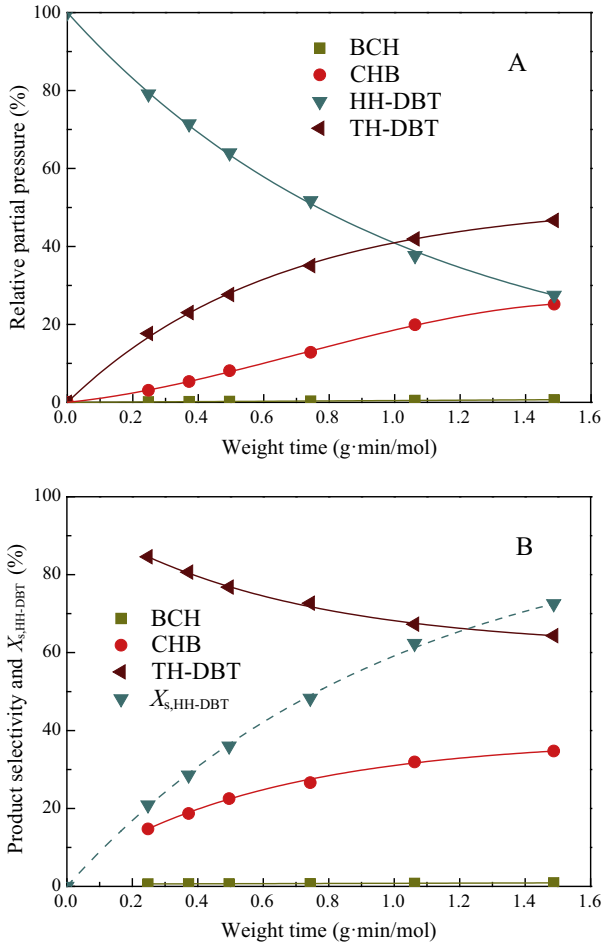

Fig. 11. HDS of HH-DBT over bulk WP at 340 °C and 0.2 kPa piperidine as a function of weight time. (A) Relative partial pressures of the reactant and products. (B) The conversion of HH-DBT ($X_{s,HH\text{-}DBT}$, dashed line) and the product selectivities (solid lines).

piperidine, no toluene or MCH could be observed. The formation of CHB and BCH in the HDS of HH-DBT (Fig. 11) and that of DM-CHB, DM-BCH, and DMDBTs in the HDS of HH-4,6-DMDBT (Fig. 12) were much more inhibited than the dehydrogenation of HH-DBT to TH-DBT or that of HH-4,6-DMDBT to TH-4,6-DMDBT, respectively. As a consequence, TH-DBT became the most abundant product in the HDS of HH-DBT (Fig. 11), while TH-4,6-DMDBT was the dominant product in the HDS of HH-4,6-DMDBT at 0.2 kPa piperidine (Fig. 12), and the yields of both main products increased continuously with weight time (Figs. 11A and 12A). After the addition of piperidine, the selectivities of 2,6-DMDBT and 3,6-DMDBT in the reaction of HH-4,6-DMDBT decreased, and, thus, that of 4,6-DMDBT increased (Table S1 in the Supplementary Material).

3.5. Hydrogenation reactions

BP reacted slowly and, at τ = 1.5 g min/mol and 0.5 kPa BT, its conversion was 9.7% with CHB as the only product. CHB reacted very slowly, and its conversion was less than 1.5%. This means that the further hydrogenation of CHB over WP was negligible in the presence of sulfur-containing compounds. DM-BP reacted much faster than BP and had a conversion of 42.5% at τ = 1.5 g min/mol and 0.5 kPa DBT (Fig. S5 in the Supplementary Material). The major product was DM-CHB. DM-BCH, toluene, and MCH were detected at very low yields (each less than 3%), and the toluene/MCH ratio was close to one. 3,4′-DM-CHB was very reactive in the presence of DBT (Fig. 13). However, it was not hydrogenated to 3,4′-DM-BCH but hydrocracked to toluene, MCH, 1-methylcyclohexene (MCHE), and a small amount of ethylcyclopentane (ECP). Combined with the very low hydrogenation reactivity of CHB, this suggests that WP has very low activity for the hydrogenation of monoaromatic rings. Thus, BCH and DM-BCH must be the products of the HDS of dodecahydrodibenzothiophene (DH-DBT) and DH-4,6-DMDBT, respectively. This agrees with results obtained over Ni_2P and MoP [10–12].

Of the products of the hydrocracking of 3,4′-DM-CHB, MCHE showed a maximum yield at τ = 0.74 g min/mol (Fig. 13A) and a nonzero initial selectivity (Fig. 13B), indicating that it was a primary product and an intermediate in the reaction of 3,4′-DM-CHB. Toluene exhibited a nearly constant selectivity of about 50%, demonstrating that its further reaction was very slow. MCH was the product of the hydrogenation of MCHE because the selectivity of MCHE decreased with weight time while that of MCH increased. ECP can be formed by the isomerization of MCH or by the hydrogenation of ethylcyclopentene, the product of the isomerization of MCHE.

4. Discussion

4.1. Comparison of the hydrodesulfurization performance of Ni_2P, MoP, and WP

The HDS of DBT, 4,6-DMDBT, and their hydrogenated intermediates over bulk Ni_2P [10,12] as well as that of DBT, TH-DBT, and

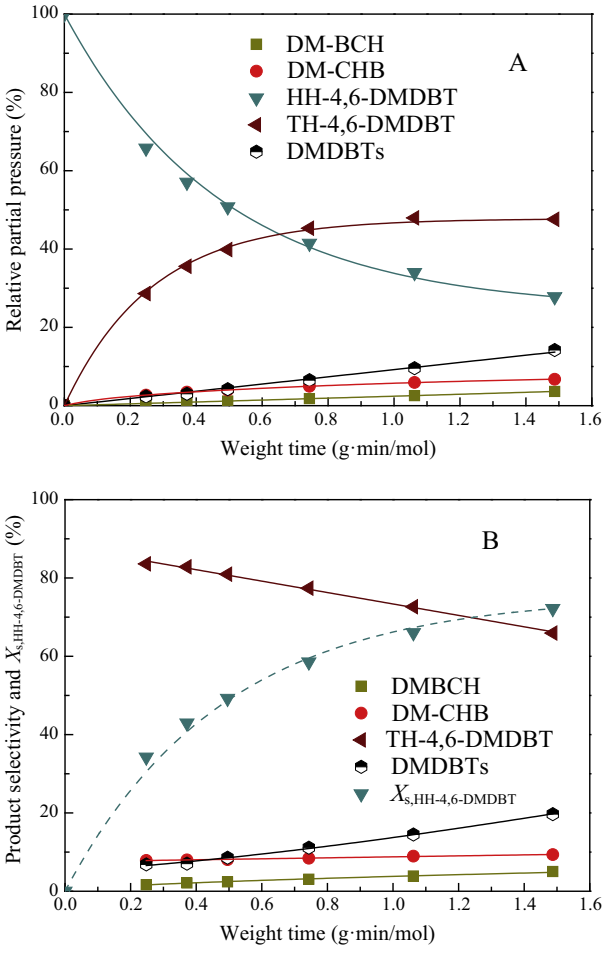

Fig. 12. HDS of HH-4,6-DMDBT over bulk WP at 340 °C and 0.2 kPa piperidine as a function of weight time. (A) Relative partial pressures of the reactant and products. (B) The conversion of HH-4,6-DMDBT ($X_{s,HH\text{-}4,6\text{-}DMDBT}$, dashed line) and the product selectivities (solid lines).

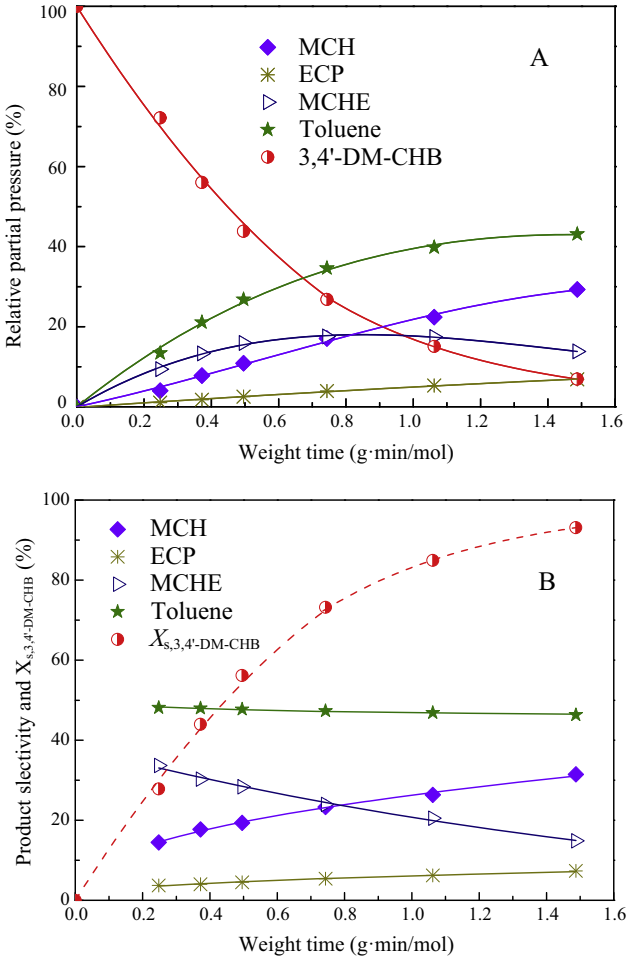

Fig. 13. The hydrogenation of 3,4′-DM-CHB over bulk WP at 340 °C and 0.5 kPa DBT as a function of weight time. (A) Relative partial pressures of the reactant and products. (B) The conversion of 3,4′-DM-CHB ($X_{s,3,4'\text{-}DM\text{-}CHB}$, dashed line) and the product selectivities (solid lines).

HH-DBT over bulk MoP [11], has been studied under reaction conditions almost identical to those in the present work. This allows a detailed comparison of the HDS performance of Ni_2P, MoP, and WP. It should be addressed that the bulk Ni_2P catalyst was synthesized with P in excess (Ni/P molar ratio of 1.0) [10]. The hydrogenation/dehydrogenation activity of WP is stronger than that of Ni_2P and MoP, as can be concluded from the following facts. First, DBT mainly desulfurizes by the DDS pathway over bulk Ni_2P [10], while the HYD pathway and DDS pathway play an equally important role in the HDS of DBT over MoP [11]. Over WP, the selectivity of BP was only about 30% (Fig. 2B), indicating that HYD is the dominant pathway. Second, TH-DBT was dehydrogenated to DBT over WP (Figs. 5, 7 and 9), but not over Ni_2P or MoP [10,11]. Third, TH-4,6-DMDBT was readily dehydrogenated to DMDBTs over WP. At low weight time, DMDBTs was the most abundant compound, and its yield passed through a maximum in the HDS of TH-4,6-DMDBT (Fig. 6) and HH-4,6-DMDBT (Fig. 10). Over Ni_2P, the yield of DMDBTs increased with weight time and did not reach its maximum at τ = 1.5 g min/mol, demonstrating that the reaction between TH-4,6-DMDBT and DMDBTs was far from equilibrium [12]. Fourth, BP and DM-BP were hydrogenated over WP in the presence of sulfur-containing compounds. This may explain the gradual decrease in the selectivities of BP and DM-BP with increasing weight time in the HDS of DBT and 4,6-DMDBT, respectively (Figs. 2 and 3). However, the hydrogenation of BP over Ni_2P [10] and MoP [11] and that of DM-BP over Ni_2P [12] were negligible under the same reaction conditions.

Generally, the thiophenic compounds are assumed to follow pseudo-first-order kinetics during HDS [26–28], and the reaction orders of the total reaction as well as of the DDS and HYD pathways are one [28]. However, it should be noted that the kinetics of the HDS of the sulfur-containing compounds is complicated. The first-order model is primitive and is a simplification under specified conditions. As pointed by Cho et al. [29], although the first-order assumption is common, it can miss essential steps in the reaction pathway by not considering surface species. Moreover, the first-order assumption did not consider the different adsorption behaviors of DBT, 4,6-DMDBT, and their hydrogenated intermediates [30]. Previously, we studied the kinetics of the HDS of DBT over the supported Co–Mo sulfides [28]. A comparison of the Langmuir–Hinshelwood (L–H) model with the pseudo-first-order model revealed that the more complicated rate expression of the L–H model can be simplified to an expression for a first-order reaction if the concentration of DBT was relatively low and the surface of the catalyst was almost bare, as in a typical commercial hydrotreating process as well as in our case at high temperature (340 °C). In the present study, all the reaction conditions were chosen carefully according to our previous work [28] to avoid the external mass transfer limitation. Moreover, we studied the influence of the size of the catalyst particles on the HDS of TH-4,6-DMDBT at τ = 1.1 g min/mol and 0 kPa piperidine (Table S2 in the Supplementary Material). Under the conditions, the conversion of TH-4,6-DMDBT was as high as 90%. The

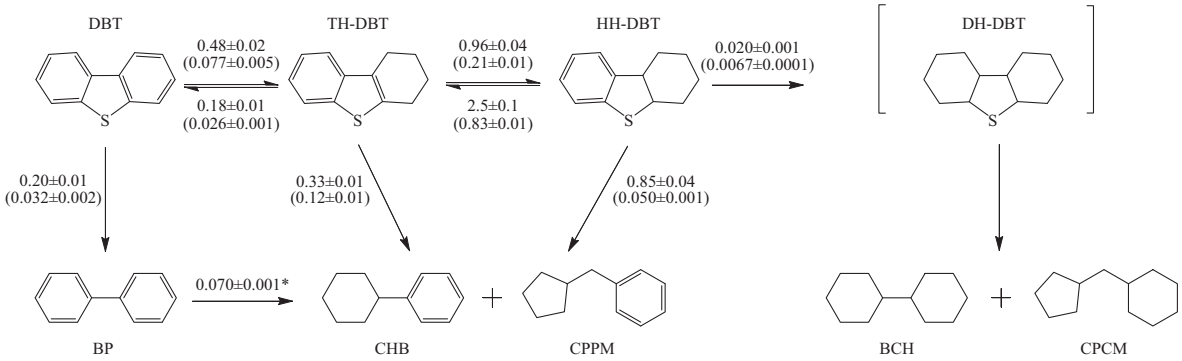

Scheme 1. Pseudo-first-order rate constants (in mol/(g min)) in the reaction network of the HDS of DBT over WP at 340 °C and 4.0 MPa in the absence or presence (in parentheses) of 0.2 kPa piperidine. * In the presence of 0.5 kPa BT.

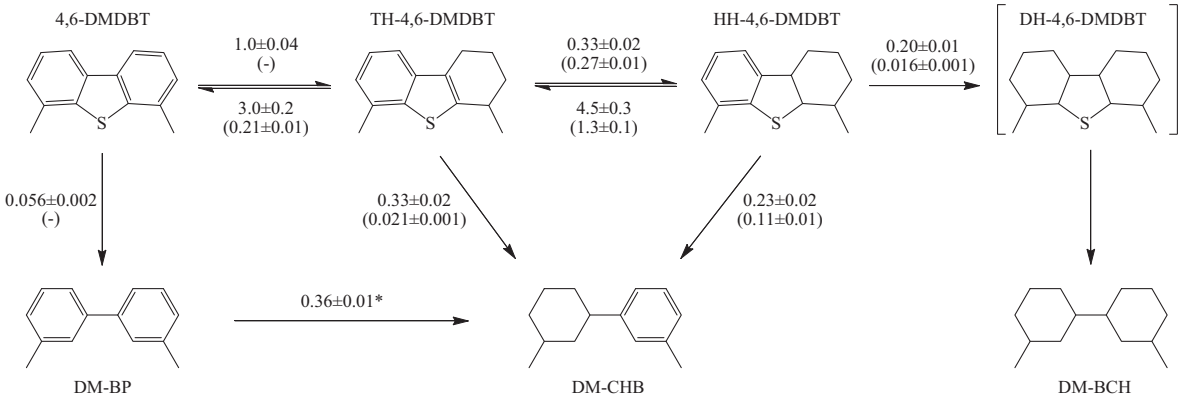

Scheme 2. Pseudo-first-order rate constants (in mol/(g min)) in the reaction network of the HDS of 4,6-DMDBT over WP at 340 °C and 4.0 MPa in the absence or presence of 0.2 kPa piperidine (in parentheses). –: completely inhibited by 0.2 kPa piperidine at $\tau \leqslant 1.1$ g min/mol; *: in the presence of 0.5 kPa DBT.

conversion of TH-4,6-DMDBT was hardly changed over these WP catalysts, suggesting that the mass transfer limitation is negligible when the particle size is less than 16 mesh (1.18 mm). Thus, all our experimental conversion data for the HDS of DBT, 4,6-DMDBT, and their hydrogenated intermediates, as well as the hydrogenation of BP and DM-BP, over WP were fitted with the pseudo-first-order model (Figs. S6–S8 in the Supplementary Material). The regression analysis indicate that the HDS of DBT and TH-DBT (Fig. S6 in the Supplementary Material) and the hydrogenation reactions (Fig. S8 in the Supplementary Material) can be reasonably fitted ($R^2 > 0.95$), whereas good fits were obtained only at short weight time ($\tau < 0.74$ g min/mol) for the HDS of HH-DBT (Fig. S6 in the Supplementary Material) and that of 4,6-DMDBT and its hydrogenated intermediates (Fig. S7 in the Supplementary Material). Such deviations at high weight time should be due to the effect of conversion. Taking TH-4,6-DMDBT (Fig. 6) and HH-DBT (Fig. 9) as examples, the conversions of the two compounds at $\tau > 0.74$ g min/mol were both higher than 85%, and the equilibrium between TH-4,6-DMDBT and 4,6-DMDBT and that between HH-DBT and TH-DBT were almost reached under the conditions. This means that the corresponding reverse reactions cannot be neglected at high weight time. Additionally, the inhibitory effect of H_2S may become significant at high conversion. Therefore, the conversions of HH-DBT and TH-4,6-DMDBT were lower than the values estimated by the pseudo-first-order model at $\tau > 0.74$ g min/mol (Figs. S6 and S7 in the Supplementary Material). Evidence is that in the presence of piperidine, when the conversion of TH-4,6-DMDBT (Fig. 8) and HH-DBT (Fig. 11) was suppressed, the experimental data of the HDS of HH-DBT and of TH-4,6-DMDBT can be well fitted to the pseudo-first-order model (Figs. S6 and S7 in the Supplementary Material). Hence, to simplify the kinetic calculations and to compare the HDS performance of WP with that of Ni_2P, MoP, and the metal sulfides reported in previous publications, we calculated the rate constants of the HDS of DBT, 4,6-DMDBT, and their hydrogenated intermediates from the experimental data at short weight time ($\tau < 0.74$ g min/mol) by assuming pseudo-first-order kinetics and by taking the hydrogenation of BP and DM-BP into account. These rate constants are valuable for a semiquantitative comparison, but it should be mentioned that they are valid only at short weight times ($\tau < 0.74$ g min/mol). The results are shown in Schemes 1 and 2.

To compare the intrinsic activity of Ni_2P, MoP, and WP, the rate constants of some steps in the networks of the HDS of DBT and 4,6-DMDBT over the catalysts were normalized by dividing the corresponding rate constants by the CO uptake of each catalyst [31]. Based on the available data shown in Table 2, the active-site-based rate constants of the hydrogenation/dehydrogenation reactions over WP were all higher than those over Ni_2P and MoP, confirming that WP possesses a higher hydrogenation/dehydrogenation activity than Ni_2P and MoP. For instance, the active-site-based rate constant of DBT to TH-DBT over WP was about 2 and 4 times larger than those over MoP and Ni_2P, respectively. In the HDS of 4,6-DMDBT, the active-site-based rate constant of 4,6-DMDBT to TH-4,6-DMDBT over WP was one order of magnitude larger than that over Ni_2P. On the other hand, the active-site-based rate constant of the DDS of DBT decreased in the order Ni_2P > MoP > WP. The intrinsic DDS activity of WP in the HDS of DBT was close to that of MoP. Nevertheless, as shown in Table 2, the active-site-based rate constant of the DDS of 4,6-DMDBT over the bulk Ni_2P catalyst was one order of magnitude lower than that over the bulk WP catalyst. Although we cannot

Table 2
The active-site-based rate constants of some reactions (in mol/(μmol min)) in the network of the HDS of DBT and 4,6-DMDBT over Ni_2P, MoP, and WP at 340 °C and total pressure 4.0 MPa in the absence or presence of piperidine (partial pressure in kPa).

	Ni_2P			MoP		WP	
	0 kPa	0.25 kPa	0.5 kPa	0 kPa	0.25 kPa	0 kPa	0.2 kPa
Hydrogenation/dehydrogenation reactions							
DBT → TH-DBT	0.056	–	0.012	0.09	0.023	0.20	0.032
TH-DBT → DBT	0	0	0	0	0	0.075	0.011
TH-DBT → HH-DBT	–	–	–	0.18	0.10	0.4	0.087
HH-DBT → TH-DBT	–	–	–	0.8	0.52	1.0	0.35
4,6-DMDBT → TH-4,6-DMDBT	0.043	0.017	–	–	–	0.42	0
TH-4,6-DMDBT → 4,6-DMDBT	0.038	0.021	–	–	–	1.3	0.087
TH-4,6-DMDBT → HH-4,6-DMDBT	0.11	0.057	–	–	–	0.14	0.11
HH-4,6-DMDBT → TH-4,6-DMDBT	0.49	0.13	–	–	–	1.9	0.54
DDS of DBT and 4,6-DMDBT							
DBT → BP	0.28	–	0.17	0.13	0.068	0.083	0.013
4,6-DMDBT → DM-BP	0.0023	0.0013	–	–	–	0.023	0

Note: –, not available.

give a definite explanation for the low DDS activity of the bulk Ni_2P in the HDS of 4,6-DMDBT at present, it should be noted that the Ni_2P catalyst was prepared with phosphorus in excess (Ni/P molar ratio of 1.0) [10], whereas a stoichiometric W/P ratio (1.0) was adopted for the synthesis of the bulk WP catalyst. The XPS characterization revealed that the surface W/P ratio (0.85) was close to the stoichiometric value. According to Oyama et al. [25], the Ni_2P active phase can be blocked by excess phosphorus at high phosphorus content. Thus, our results seem to suggest that this blocking effect is particularly pronounced for the HDS of 4,6-DMDBT over the bulk Ni_2P catalyst.

4.2. Hydrodesulfurization kinetics and the effect of methyl groups

In the network of the HDS of DBT in the absence of piperidine (Scheme 1), both the hydrogenation of TH-DBT to HH-DBT and the reverse dehydrogenation of HH-DBT to TH-DBT were very fast, the dehydrogenation being fastest. The reaction of HH-DBT to BCH and CPCM was the slowest step. This must be due to the slow hydrogenation of HH-DBT to DH-DBT, because the desulfurization of DH-DBT is very fast [30]. In the absence of piperidine, the hydrogenation of DBT to TH-DBT (0.48 mol/g min) was 24 times faster than the hydrogenation of HH-DBT to DH-DBT (0.02 mol/g min), demonstrating that over WP, hydrogenation of the second phenyl ring is much more difficult than that of the first phenyl ring. The same result was obtained over Ni_2P [10], MoP [11], and conventional sulfide catalysts [13,17,32], which can be attributed to the lower resonance energy of a multiring aromatic system than of a monoaromatic ring. The dehydrogenation of TH-DBT to DBT was about as fast as the DDS of DBT. The desulfurization rates decreased in the order HH-DBT (0.85 mol/g min) > TH-DBT (0.33 mol/g min) > DBT (0.20 mol/g min). This order is the same as that observed over Ni_2P [10], but different from that over metal sulfides. Over a Ni–MoS_2/Al_2O_3 catalyst at 300 °C and 3 MPa, the desulfurization rates for DBT, TH-DBT, and HH-DBT were in the order DBT > TH-DBT > HH-DBT [13], while over a Co–MoS_2/Al_2O_3 catalyst the order was DBT ≫ TH-DBT > HH-DBT [32]. One explanation could be that the desulfurization of HH-DBT over WP follows a different mechanism than that of DBT and TH-DBT. Over Ni_2P, we found that DBT and TH-DBT underwent desulfurization mainly through hydrogenolysis, while the desulfurization of HH-DBT occurred via β-elimination [10]. At present, we cannot explain why metal sulfides behave differently in the HDS reactions from the metal phosphides. Nevertheless, it should be noted that the nature of the metal sulfides is different from that of the metal phosphides. Metal sulfides such as MoS_2 and WS_2 are semiconductors, whereas metal phosphides are metals.

The methyl groups at the 4 and 6 positions significantly enhanced the hydrogenation rate of 4,6-DMDBT and the dehydrogenation rates of TH-4,6-DMDBT and HH-4,6-DMDBT, but decreased the rate of hydrogenation of TH-4,6-DMDBT to HH-4,6-DMDBT. In the network of the HDS of 4,6-DMDBT at 0 kPa piperidine (Scheme 2), the dehydrogenation of HH-4,6-DMDBT to TH-4,6-DMDBT was the fastest step, and its rate constant (4.5 mol/g min) was 1.8 times higher than that of the dehydrogenation of HH-DBT to TH-DBT (2.5 mol/g min, Scheme 1). The dehydrogenation of TH-4,6-DMDBT became the second fastest step. It was about 17 times faster than the dehydrogenation of TH-DBT to DBT. This explains why the DMDBTs were the most abundant products at short weight times in the HDS of TH-4,6-DMDBT and HH-4,6-DMDBT (Figs. 6 and 10). Over bulk Ni_2P, we also observed fast dehydrogenation of TH-4,6-DMDBT to DMDBTs [12], but no dehydrogenation of TH-DBT to DBT under the same conditions [10]. Thus, the dehydrogenation of TH-4,6-DMDBT is much faster than that of TH-DBT.

We therefore calculated the thermodynamics of the hydrogenation of 4,6-DMDBT to TH-4,6-DMDBT and DBT to TH-DBT under standard conditions by the DFT method at the B3LYP/6-31G* level. This method has been employed by Chen et al. for the calculation of the thermodynamics of DBT [33]. The $-\Delta_f G^0$ obtained for the hydrogenation of DBT was 22.8 kJ/mol, much higher than that for the hydrogenation of 4,6-DMDBT (7.1 kJ/mol) (Table S3 in the Supplementary Material). The partial pressure of 4,6-DMDBT is thus expected to be higher than that of DBT under equilibrium conditions.

The hydrogenation of HH-4,6-DMDBT and the subsequent desulfurization of DH-4,6-DMDBT to DM-BCH (0.2 mol/g min) were one order of magnitude faster than that of HH-DBT to BCH (0.02 mol/g min), and this was no longer the slowest step in the network of the HDS of 4,6-DMDBT. Instead, the DDS of 4,6-DMDBT was the slowest due to the steric hindrance caused by the methyl groups. Its rate constant (0.06 mol/g min) was about four times smaller than the DDS of DBT (0.2 mol/g min). However, the rate of the HYD of 4,6-DMDBT (1.0 mol/g min) was two times faster than the hydrogenation of DBT (0.48 mol/g min, Scheme 1). Because the HYD pathway is more important than the DDS pathway in the HDS of DBT and 4,6-DMDBT over bulk WP, the consequence of the increase in the rate of the HYD pathway is that 4,6-DMDBT is more reactive than DBT. As shown in Figs. 2 and 3, 4,6-DMDBT exhibited higher conversion than DBT, and the yields of DM-CHB and DM-BCH (the products of the HYD pathway of 4,6-DMDBT) were larger than those of CHB and BCH (the products of the HYD pathway of DBT). For reference, the turnover frequencies (TOFs) of DBT and 4,6-DMDBT at short weight time

(0.37 g min/mol) over WP, Ni_2P, and MoP were all calculated (Table S4 in the Supplementary Material). Over Ni_2P, as generally accepted, the TOF of 4,6-DMDBT in the absence of piperidine was much lower than that of DBT. However, 4,6-DMDBT showed a higher TOF than DBT at 0 kPa piperidine. These results suggest that WP is particularly promising for deep HDS. Not only the hydrogenation of the sulfur-containing compounds, but also that of DM-BP, was accelerated by the methyl groups. The rate of hydrogenation of DM-BP in the presence of 0.5 kPa DBT (0.36 mol/g min) was five times as fast as that of BP at 0.5 kPa BT (0.07 mol/g min), demonstrating that the hydrogenation of DM-BP cannot be neglected in the HDS of 4,6-DMDBT. Also, over a Ni–MoS_2/γ-Al_2O_3 catalyst, the methyl groups promoted the hydrogenation of 4,6-DMDBT, TH-4,6-DMDBT, and HH-4,6-DMDBT; this was suggested to be the result of electron donation by the methyl groups [13].

While the DDS of TH-DBT (0.33 mol/g min) was 2.6 times slower than that of HH-DBT (0.85 mol/g min) (Scheme 1), the DDS of TH-4,6-DMDBT (0.33 mol/g min) was faster than that of HH-4,6-DMDBT (0.23 mol/g min) (Scheme 2). This is in agreement with results reported for the HDS of DBT, 4,6-DMDBT, and their hydrogenated intermediates over metal sulfides [13,32]. At 300 °C and total pressure 3 MPa, the rate constants of the DDS of TH-4,6-DMDBT and HH-4,6-DMDBT over a Ni–MoS_2/γ-Al_2O_3 catalyst were 0.23 kPa mol/g min and 0.21 kPa mol/g min, respectively [13]. Over a Co–MoS_2/γ-Al_2O_3 catalyst under identical conditions, the obtained rate constants of DDS of TH-DBT and HH-DBT were 0.13 and 0.10 mol/g min, respectively [32]. Sun and Prins suggested that the removal of the sulfur atom from these molecules over metal sulfides proceeds by a hydrogenolysis reaction through a late transition state, determined by formation of a carbon–metal bond, rather than through an early transition state, determined by breaking of the carbon–sulfur bond [32]. In other words, the hydrogenation weakens one of the C–S bonds in the DBT molecule, but aryl–metal bonds are more stable than alkyl–metal bonds [32]. Thus, the fact that the rate constant of the desulfurization of TH-4,6-DMDBT to DM-CHB is higher than that of HH-4,6-DMDBT to DM-CHB would suggest that the desulfurization of TH-4,6-DMDBT and HH-4,6-DMDBT over WP does not proceed through elimination, but through hydrogenolysis.

Our results thus suggest that the methyl groups in 4,6-DMDBT, TH-4,6-DMDBT, and HH-4,6-DMDBT have several effects. They not only provide strong steric hindrance for the direct removal of the sulfur atom and substantially accelerate the hydrogenation/dehydrogenation of the compounds, but also affect the modes of cleavage of the C–S bonds in HH-DBT and HH-4,6-DMDBT. The steric hindrance and few β-hydrogen atoms could explain why hydrogenolysis is preferred for the cleavage of the cycloalkyl C–S bond in HH-4,6-DMDBT over WP. To fully understand the role the methyl groups, further experimental and theoretical work and better insight into the nature of the active site(s) of WP are required.

4.3. The inhibitory effect of piperidine

All steps in the networks of the HDS of DBT and 4,6-DMDBT were strongly inhibited by piperidine (Schemes 1 and 2). Over the bulk WP catalyst, the DDS and HYD pathways of DBT were about equally inhibited by piperidine. The rate constants of these two pathways were both about six times lower in the presence than in the absence of piperidine. This is different from the cases over metal sulfides [34–36] as well as over bulk Ni_2P [10] and bulk MoP catalysts [11]. Over these catalysts, the HYD pathway of DBT was more strongly inhibited by nitrogen-containing compounds than the DDS pathway. The reaction of 4,6-DMDBT was much more strongly inhibited by piperidine than that of DBT. The conversion of 4,6-DMDBT was completely inhibited by 0.2 kPa piperidine at $\tau \leqslant 1.1$ g min/mol. Only when piperidine was almost completely converted at $\tau = 1.5$ g min/mol (Fig. S4 in the Supplementary Material) did 4,6-DMDBT start to react. Therefore, we did not calculate the rate constants of its HYD and DDS pathways. The overall active-site-based rate constant of the HDS of DBT in the absence of piperidine over WP (0.28 mol/μmol min) was comparable to that over Ni_2P (0.336 mol/μmol min) and higher than that over MoP (0.22 mol/μmol min) (Table 2). For the HDS of 4,6-DMDBT, the overall active-site-based rate constant over WP (0.44 mol/μmol min) was 10 times higher than over Ni_2P (0.045 mol/μmol min) (Table 2), indicating that the intrinsic activity of WP in the HDS of 4,6-DMDBT is much higher than that of Ni_2P. However, the situation was reversed after the addition of piperidine. For the HDS of DBT, WP became the least active catalyst (Table 2). Ni_2P was more nitrogen-tolerant than WP and MoP. Even in the presence of 0.5 kPa piperidine, Ni_2P was still the most active catalyst in catalyzing the HDS of DBT (Table 2). The variations of the TOFs of DBT and 4,6-DMDBT over Ni_2P, MoP, and WP (Table S4 in the Supplementary Material) agreed with these results. At $\tau = 0.37$ g min/mol, the TOF of 4,6-DMDBT over WP decreased to zero after the addition of piperidine. Thus, WP is more sensitive to piperidine than Ni_2P and MoP. This may explain why, although WP is superior to Ni_2P in the HDS of 4,6-DMDBT in the absence of piperidine, its activity in simultaneous HDS and HDN is lower than that of Ni_2P [5,6]. The inhibitory effect of nitrogen-containing compounds on HDS is usually ascribed to their competitive adsorption with sulfur-containing compounds. If the same holds true for WP, the adsorption of piperidine onto WP should be much stronger than that of DBT and 4,6-DMDBT. Since the HDS of 4,6-DMDBT was more inhibited by piperidine than that of DBT, the adsorption of 4,6-DMDBT over WP is expected to be weaker than that of DBT.

The degree of inhibition of piperidine on the DDS of 4,6-DMDBT and its hydrogenated intermediates was in the order 4,6-DMDBT $\gg$ TH-4,6-DMDBT > HH-4,6-DMDBT. This must be due to the different adsorption constants of these molecules. As discussed above, the DDS of 4,6-DMDBT, TH-4,6-DMDBT, and HH-4,6-DMDBT may occur mainly through hydrogenolysis over WP. A prerequisite for the hydrogenolysis of the aromatic sulfides over metal sulfides or metals is the perpendicular adsorption of these molecules onto the active site through the sulfur atom (σ-adsorption). Hydrogenation of a phenyl ring increases the electron density on the sulfur atom, and thus increases the interaction with the active sites of the catalyst [37]. Thus, the DDS of HH-4,6-DMDBT was less inhibited by piperidine than the DDS of TH-4,6-DMDBT and 4,6-DMDBT over WP. However, as shown in Scheme 1, the inhibition of piperidine was much stronger on the DDS of HH-DBT than on the DDS of DBT or TH-DBT. This might be another indication that the DDS of HH-DBT occurs through a different mechanism. According to our previous work [10], the desulfurization of HH-DBT over WP most likely proceeds by β-elimination. Two types of active sites are required for β-elimination: a basic site to abstract the β-hydrogen atom and an acid or vacancy site to bind the sulfur atom of the reactant [38]. The acid or vacancy sites can be severely poisoned by piperidine, because it is a strong base.

Piperidine had a different effect on the dehydrogenation of HH-DBT or HH-4,6-DMDBT and the hydrogenation of TH-DBT or TH-4,6-DMDBT (Schemes 1 and 2), which was also observed over Ni_2P [12]. The equilibrium between the tetrahydro and hexahydro intermediates should not be affected by an inhibitor. An explanation could be that different amounts of the four HH-4,6-DMDBT isomers (4,4a-trans;4a,9b-cis, 4,4a-trans;4a,9b-trans, 4,4a-cis;4a,9b-cis, and 4,4a-cis;4a,9b-trans) were present in the reaction products, which may complicate the thermodynamics [12]. Once we have prepared large enough amounts of the pure isomers of HH-4,6-DMDBT and HH-DBT, this question can be studied further.

4.4. The metallic character of tungsten phosphide and the cleavage of the cycloalkyl C–S bond

Over Ni_2P, minor amounts of two isomers of 4,6-DMDBT (2,6-DMDBT and 3,6-DMDBT) were detected in the reaction products of TH-4,6-DMDBT and HH-4,6-DMDBT [12]. Because the acidity of Ni_2P was too weak to catalyze the skeletal isomerization of alkenes, it was suggested that the methyl group migration was due to the metallic character of Ni_2P [12]. The reason is that not only acid sites but also metal surfaces are able to catalyze skeletal rearrangements of hydrocarbons [39,40]. Also, in the present study, 2,6-DMDBT and 3,6-DMDBT were detected, with selectivities (Table S1 in the Supplementary Material) similar to those over Ni_2P [12]. The NH_3-TPD results (Fig. S3 in the Supplementary Material) show that the acidity of WP was weak. To evaluate the acidity of WP at the working temperature, the isomerization of 1-heptene was carried out at 340 °C and τ = 1.5 g min/mol over WP and quartz sand (as reference). The results (Table S5 in the Supplementary Material) indicate that the selectivity of the skeletal isomerization products was as low as 0.7% at a 1-heptene conversion of 84.8% over WP. Over quartz sand, the conversion of 1-heptene was 51.3%, and the selectivity of skeletal isomerization was 0.1%. Thus, the skeletal isomerization of 1-heptene was negligible over WP, demonstrating that WP had very low acidity. This also means that the cracking of 3,4′-DM-CHB observed in its hydrogenation over WP (Fig. 13) cannot be attributed to the acidity of WP, because cracking requires stronger acidity than skeletal isomerization [41,42]. Therefore, since both the skeletal isomerization and hydrocracking of hydrocarbons can be catalyzed by a metal surface [39], we suggest that both the methyl group migration in the dehydrogenation of TH-4,6-DMDBT and the hydrocracking of 3,4′-DM-CHB are due to the metallic nature of WP. The metallic character of WP has been proved by NMR and DFT calculations. Oyama et al. [43] attributed the large shift in the ^{31}P NMR spectrum of WP to a Knight shift, because of the metallic character of WP. Joshi et al. [44] reported that the metallic behavior of WP was due to crossover of the Fermi level by bands originated from 3*p* states of P and 5*d* states of W. To verify this assumption, we studied the hydrogenation of 3,4′-DM-CHB over a Pd/SiO_2 catalyst under exactly the same reaction conditions as over the WP catalyst (Fig. S9 in the Supplementary Material). The hydrogenation of 3,4′-DM-CHB to 3,4′-DM-BCH and the hydrocracking to toluene, MCH, and MCHE occurred simultaneously over the Pd/SiO_2 catalyst, with similar total product selectivities. No ECP was detected. The distributions of toluene, MCH, and MCHE over Pd/SiO_2 were similar to those over WP (Fig. 13), and the ratio of the selectivity of toluene to the total selectivity of MCH and MCHE was close to 1. The hydrocracking of hydrocarbons over transition metals could be interpreted in terms of metallocarbene chemistry [39]. Gault [39] attributed the different product distributions in the isomerization and hydrocracking of 2- and 3-methylpentanes over Pd, Pt, Ir, Ni, and Co to their different capacities to form metallocarbenes. Over WP, only 3,4′-DM-CHB underwent hydrocracking, whereas CHB was very stable. This suggests that methyl groups would significantly promote the formation of metallocarbene intermediate between WP and 3,4′-DM-CHB or decrease the stability of 3,4′-DM-CHB.

The above discussion suggests that the CPPM and CPCM detected in the HDS of DBT, TH-DBT, and HH-DBT (Figs. 2, 5 and 9) originate from the isomerization of the corresponding hydrocarbons over WP due to its metallic character. The low activity of WP in the hydrogenation of the monoaromatic ring rules out BCH and CPCM having been formed by the hydrogenation of CHB and CPPM, respectively, during the HDS of DBT, TH-DBT, and HH-DBT. Also, in the presence of benzothiophene, CHB showed a very low hydrogenation reactivity over WP and BCH was the only product. This suggests that CPPM cannot be the product of the isomerization of CHB. We therefore investigated the hydrogenation of 1-phenyl-1-cyclohexene (1-PCHE) and 3-phenyl-1-cyclohexene (3-PCHE) in the absence and presence of 35 kPa H_2S at τ = 1.5 g min/mol. These two compounds are the intermediates of the desulfurization of TH-DBT and HH-DBT to CHB [10,17]. H_2S was added because sulfur plays an important role in HDS over transition-metal phosphides. A surface metal phosphosulfide generated during HDS reactions has been established as the real active phase for working Ni_2P and MoP catalysts [1,11,24,45]. As one of the HDS products and an acid, H_2S could influence the active sites of WP or directly participate in the reactions, which allows the isomerization of the hydrocarbons and the formation of CPPM and CPCM. The results summarized in Table S6 (Supplementary Material) indicate that 1-PCHE and 3-PCHE were very reactive, and complete conversion was achieved in the absence and in the presence of H_2S. CHB was the major product, with a yield around 83% at 0 kPa H_2S. CPPM and CPCM were indeed detected in the absence of H_2S. However, their yields were lower than in the HDS of HH-DBT (Fig. 9). No CPCM was observed in the presence of H_2S, because the hydrogenation of CHB to BCH was strongly inhibited by H_2S. This also means that isomerization of BCH into CPCM does not take place and that H_2S does not lead to the formation of acidic sites. The CHB/CPPM ratio varied from 21.0 (starting from 1-PCHE) or 22.7 (starting from 3-PCHE) at 0 kPa H_2S to 24.7 or 18.5 at 35 kPa H_2S, respectively. Assuming that CHB detected in the HDS of HH-DBT was derived solely from the hydrogenation of phenylcyclohexene and taking the smallest CHB/CPPM ratio of 18.7, the maximum yield of CPPM in the HDS of HH-DBT at τ = 1.5 g min/mol is estimated to be 2.4% (45.4%/18.7), which is only half of the experimental value (4.7%). Furthermore, the yield of CPCM in the hydrogenation of 1-PCHE and 3-PCHE was lower than that of BCH (Table S6 in the Supplementary Material). This disagrees with the HDS of DBT, TH-DBT, and HH-DBT, where the yield of CPCM was comparable to that of BCH (Figs. 2, 5 and 9), suggesting that the isomerization of the corresponding hydrocarbons over WP is not the only mechanism for the formation of CPCM and CPPM.

Another possibility for accounting for the formation of CPCM and CPPM is the heterolytic cleavage of the cycloalkyl C–S bonds in HH-DBT and DH-DBT. For instance, the heterolytic cleavage of the cycloalkyl C–S bond of HH-DBT leads to the formation of a RS^- anion and a carbocation (Scheme S1 in the Supplementary Material). Elimination of the β hydrogen atom attached to C(9b) or C(4) produces 1-PCHE and 3-PCHE, respectively, and the subsequent desulfurization and hydrogenation yield CHB. The creation of the carbocation will allow a skeletal isomerization of the ring, and the final product of this pathway could be CPPM (Scheme S1 in the Supplementary Material). When DH-DBT is the reactant, BCH and CPCM can be formed. This mechanism is based on the E1 elimination reaction, with sulfur as the leaving group. Surface defects or vacancies may act as active sites to accommodate sulfur [38], while the negatively charged surface sites (e.g., P sites) or even formed S^- anions might be the base that eliminates the β hydrogen. This may explain why no corresponding skeletal isomers of DM-CHB and DM-BCH were detected in the HDS of 4,6-DMDBT and its hydrogenated intermediates. As discussed in Sections 4.2 and 4.3, the desulfurization of 4,6-DMDBT, TH-4,6-DMDBT, and HH-4,6-DMDBT may proceed mainly through hydrogenolysis rather than elimination. Such a heterolytic process or E1 elimination is only one of the possibilities for cleaving C–S bonds. The hydrogenolysis of TH-DBT followed by the hydrogenation of the derived phenylcyclohexene and the hydrogenolysis of HH-DBT may also contribute to the formation of CHB. This would explain why the yield of CHB was much higher than that of CPPM in the HDS of HH-DBT over bulk WP. Two other questions are why

CPPM and CPCM were not observed in the HDS of HH-DBT over Ni_2P under the same conditions [10], and why the yields of these two compounds over MoP were too low to allow a mechanistic study [11]. Apparently, WP is the most active transition-metal phosphide for the heterolytic cleavage of the cycloalkyl C–S bond. Our results suggest that the real active sites of the WP catalyst and the surface reactions must be complex. A thorough understanding of these points is needed before we can really answer these questions.

5. Conclusions

WP possesses a higher hydrogenation/dehydrogenation activity than Ni_2P and MoP. Over WP, the HDS of both DBT and 4,6-DMDBT occurred predominantly through the HYD pathway, in which the hydrogenation of BP and DM-BP cannot be neglected. The rate constants of all the steps of the kinetic networks of the HDS of DBT and 4,6-DMDBT were determined. The methyl groups at the 4 and 6 positions suppressed the direct desulfurization of 4,6-DMDBT by steric hindrance, significantly promoted the hydrogenation of 4,6-DMDBT and the dehydrogenations of TH-4,6-DMDBT and HH-4,6-DMDBT, but decreased the rate of hydrogenation of TH-4,6-DMDBT. Consequently, the total HDS reactivity of 4,6-DMDBT over WP was higher than that of DBT. WP was highly sensitive to piperidine. Piperidine inhibited the HDS of 4,6-DMDBT much more strongly than that of DBT. Substantial dehydrogenation of TH-4,6-DMDBT to 4,6-DMDBT and two of its isomers occurred. The formation of these isomers, as well as the hydrocracking of 3,4′-DM-CHB, is not due to the low acidity of WP but probably to its metallic character. Based on kinetic analysis, the mechanisms of the cleavage of the C–S bonds in these polyaromatic sulfur-containing compounds over WP were discussed. The isomerization of phenylcyclohexene isomers over WP is not sufficient to account for the formation of CPPM and CPCM. Thus, we suggested that the heterolytic cleavage (E1 elimination) of the cycloalkyl C–S bond in HH-DBT or DH-DBT should also be considered.

Acknowledgments

This work was financially supported by the Natural Science Foundation of China (21073022, 21173033, U1162203, and 21473017), the Fundamental Research Funds for the Central Universities (DUT13LK18), the PetroChina Innovation Foundation (2014D-5006-0402), the Scientific Research Fund of Liaoning Provincial Education Department (L2013023), and the State Key Laboratory of Fine Chemicals (KF1306). We thank Professor C. Hao from Dalian University of Technology, who generously offered the GAUSSIAN 03W software package for the whole computational tasks.

Appendix A. Supplementary material

Supplementary data associated with this article can be found, in the online version, at http://dx.doi.org/10.1016/j.jcat.2015.07.019.

References

[1] S.T. Oyama, J. Catal. 216 (2003) 343.
[2] S.T. Oyama, T. Gott, H. Zhao, Y.-K. Lee, Catal. Today 143 (2009) 94.
[3] R. Prins, M.E. Bussell, Catal. Lett. 142 (2012) 1413.
[4] S. Carenco, D. Portehault, C. Boissière, N. Mézailles, C. Sanchez, Chem. Rev. 113 (2013) 7981.
[5] X. Wang, P. Clark, S.T. Oyama, J. Catal. 208 (2002) 321.
[6] P. Clark, X. Wang, S.T. Oyama, J. Catal. 207 (2002) 256.
[7] H. Zhao, S.T. Oyama, H.-J. Freund, R. Wlodarczyk, M. Sierka, Appl. Catal. B: Environ. 164 (2015) 204.
[8] W. Tremel, R. Hoffmann, J. Silvestre, J. Am. Chem. Soc. 108 (1986) 5174.
[9] M. Egorova, R. Prins, J. Catal. 225 (2004) 417.
[10] X. Li, J. Bai, A. Wang, R. Prins, Y. Wang, Top. Catal. 54 (2011) 290.
[11] J. Bai, X. Li, A. Wang, R. Prins, Y. Wang, J. Catal. 287 (2012) 161.
[12] L. Yang, X. Li, A. Wang, R. Prins, Y. Wang, Y. Chen, X. Duan, J. Catal. 317 (2014) 144.
[13] H. Wang, R. Prins, J. Catal. 264 (2009) 31.
[14] H. Gilman, A.L. Jacoby, J. Org. Chem. 3 (1938) 108.
[15] J.C. DiCesare, L.B. Thompson, R.J. Andersen, J. Nail, Org. Prep. Proced. Int. 32 (2000) 169.
[16] X. Xu, X. Li, A. Wang, Y. Sun, W.B. Schweizer, R. Prins, Helv. Chim. Acta 94 (2011) 1754.
[17] H. Wang, R. Prins, J. Catal. 258 (2008) 153.
[18] O. Levenspiel, Chemical Reaction Engineering, third ed., Wiley, 1998.
[19] G.N. Koshel', S.G. Koshel', M.V. Postnova, N.V. Lebedeva, E.A. Kuznetsova, M.S. Belysheva, T.A. Yun'kova, Kinet. Catal. 45 (2004) 821.
[20] I.I. Abu, K.J. Smith, J. Catal. 241 (2006) 356.
[21] M.J. Frisch, G.W. Trucks, H.B. Schlegel, G.E. Scuseria, M.A. Robb, J.R. Cheeseman, J.A. Montgomery Jr., T. Vreven, K.N. Kudin, J.C. Burant, J.M. Millam, S.S. Iyengar, J. Tomasi, V. Barone, B. Mennucci, M. Cossi, G. Scalmani, N. Rega, G.A. Petersson, H. Nakatsuji, M. Hada, M. Ehara, K. Toyota, R. Fukuda, J. Hasegawa, M. Ishida, T. Nakajima, Y. Honda, O. Kitao, H. Nakai, M. Klene, X. Li, J.E. Knox, H.P. Hratchian, J.B. Cross, C. Adamo, J. Jaramillo, R. Gomperts, R.E. Stratmann, O. Yazyev, A.J. Austin, R. Cammi, C. Pomelli, J.W. Ochterski, P.Y. Ayala, K. Morokuma, G.A. Voth, P. Salvador, J.J. Dannenberg, V.G. Zakrzewski, S. Dapprich, A.D. Daniels, M.C. Strain, O. Farkas, D.K. Malick, A.D. Rabuck, K. Raghavachari, J.B. Foresman, J.V. Ortiz, Q. Cui, A.G. Baboul, S. Clifford, J. Cioslowski, B.B. Stefanov, G. Liu, A. Liashenko, P. Piskorz, I. Komaromi, R.L. Martin, D.J. Fox, T. Keith, M.A. Al-Laham, C.Y. Peng, A. Nanayakkara, M. Challacombe, P.M.W. Gill, B. Johnson, W. Chen, M.W. Wong, C. Gonzalez, J.A. Pople, GAUSSIAN 03, Revision B.05, Gaussian Inc., Pittsburgh, PA, 2003.
[22] C.-Y. Kim, J.W. Elam, M.J. Pellin, D.K. Goswami, S.T. Christensen, M.C. Hersam, P.C. Stair, M.J. Bedzyk, J. Phys. Chem. B 110 (2006) 12616.
[23] P. Clark, W. Li, S.T. Oyama, J. Catal. 200 (2001) 140.
[24] J. Kibsgaard, T.F. Jaramillo, Angew. Chem. Int. Ed. 53 (2014) 14433.
[25] S.T. Oyama, X. Wang, Y.-K. Lee, K. Bando, F.G. Requejo, J. Catal. 210 (2002) 207.
[26] M. Egorova, R. Prins, J. Catal. 221 (2004) 11.
[27] M.J. Girgis, B.C. Gates, Ind. Eng. Chem. Res. 30 (1991) 2021.
[28] Y. Wang, Z. Sun, A. Wang, L. Ruan, M. Lu, J. Ren, X. Li, C. Li, Y. Hu, P. Yao, Ind. Eng. Chem. Res. 43 (2004) 2324.
[29] A. Cho, H. Kim, A. Iino, A. Takagaki, S.T. Oyama, J. Catal. 318 (2014) 151.
[30] X. Li, A. Wang, M. Egorova, R. Prins, J. Catal. 250 (2007) 283.
[31] J.H. Kim, X. Ma, C. Song, Energy Fuels 19 (2005) 353.
[32] Y. Sun, R. Prins, J. Catal. 267 (2009) 193.
[33] S.D. Chen, H.X. Liu, Z.Y. Wang, J. Chem. Eng. Data 52 (2007) 1195.
[34] C. Kwack, J.J. Lee, J.S. Bae, S.H. Moon, Appl. Catal. B: Environ. 35 (2001) 59.
[35] C. Kwack, M.Y. Kim, K. Choi, S.H. Moon, Appl. Catal. A: Gen. 185 (1999) 19.
[36] V.M. Kogan, R.G. Gaziev, S.W. Lee, N.N. Rozhdestvenskaya, Appl. Catal. A: Gen. 251 (2003) 187.
[37] X. Ma, K. Sakanishi, T. Isoda, I. Mochida, Energy Fuels 9 (1995) 33.
[38] F. Bataille, J.L. Lemberton, P. Michaud, G. Pérot, M. Vrinat, M. Lemaire, E. Schulz, M. Breysse, S. Kasztelan, J. Catal. 191 (2000) 409.
[39] F.G. Gault, Adv. Catal. 30 (1981) 1.
[40] G. Maire, F. Garin, J. Mol. Catal. 48 (1988) 99.
[41] P.A. Jacobs, in: F. Delannay (Ed.), Characterization of Heterogeneous Catalysts, Dekker, New York, 1984, p. 367.
[42] D. Li, M. Li, Y. Chu, H. Nie, Y. Shi, Catal. Today 81 (2003) 65.
[43] S.T. Oyama, P. Clark, X. Wang, T. Shido, Y. Iwasawa, S. Hayashi, J.M. Ramallo-López, F.G. Requejo, J. Phys. Chem. B 106 (2002) 1913.
[44] R. Joshi, J. Sahariya, H.S. Mud, K.C. Bhamu, S. Tiwari, B.L. Ahuja, Comput. Mater. Sci. 53 (2012) 89.
[45] F. Sun, W. Wu, Z. Wu, J. Guo, Z. Wei, Y. Yang, Z. Jiang, F. Tian, C. Li, J. Catal. 228 (2004) 298.